Applied Thermal Engineering 30 (2010) 1914–1926

Contents lists available at ScienceDirect

Applied Thermal Engineering

journal homepage: www.elsevier.com/locate/apthermeng

Determination of TDC in internal combustion engines by a newly developed thermodynamic approach

Emiliano Pipitone*, Alberto Beccari

Dipartimento di Meccanica, University of Palermo, viale delle scienze, 90128 Palermo, Italy

ARTICLE INFO

Article history:
Received 9 September 2008
Accepted 9 April 2010
Available online 23 June 2010

Keywords:
Top dead centre determination
Spark ignition engine
Compression ignition engine
TDC

ABSTRACT

In-cylinder pressure analysis is nowadays an indispensable tool in internal combustion engine research & development. It allows the measure of some important performance related parameters, such as indicated mean effective pressure (IMEP), mean friction pressure, indicated fuel consumption, heat release rate, mass fraction burned, etc.. Moreover, future automotive engine will probably be equipped with in-cylinder pressure sensors for continuous combustion monitoring and control, in order to fulfil the more and more strict emission limits. For these reasons, in-cylinder pressure analysis must be carried out with maximum accuracy, in order to minimize the effects of its characteristic measurement errors. The exact determination of crank position when the piston is at top dead centre (TDC) is of vital importance, since a 1° degrees error can cause up to a 10% evaluation error on IMEP and 25% error on the heat released by the combustion: the position of the crank shaft (and hence the volume inside the cylinder) should be known with the precision of at least 0.1 crank angle degrees, which is not an easy task, even if the engine dimensions are well known: it corresponds to a piston movement in the order of one tenth of micron, which is very difficult to estimate. A good determination of the TDC position can be pursued by means of a dedicated capacitive TDC sensor, which allows a dynamic measurement (i.e. while engine is running) within the required 0.1° precision [1,2]. Such a sensor has a substantial cost and its use is not really fast, since it must be fitted in the spark plug or injector hole of the cylinder. A different approach can be followed using a thermodynamic method, whose input is in-cylinder pressure sampled during the compression and expansion strokes: some of these methods, more or less valid, can be found in literature [3–8]. This paper will discuss a new thermodynamic approach to the problem of the right determination of the TDC position. The base theory of the method proposed is presented in the first part, while the second part deals with the assessment of the method and its robustness to the most common in-cylinder pressure measurement errors.

1. Base theory of the method

The compression and expansion processes in a motored (i.e. without combustion) engine can be described observing the energy transformations regarding the unity mass which remains in the cylinder. The first law of thermodynamics states that:

$$dq - pdv = du \tag{1}$$

where dq represents the elementary specific heat received by the gas from the cylinder walls, p and v represent the gas pressure and specific volume, and u the specific internal energy.

The gas involved in the process is air and can be assumed to be a perfect gas, thus the following equations are also valid:

$$\left.\begin{aligned} p\,v &= R'T \Rightarrow \frac{dp}{p} + \frac{dv}{v} = \frac{dT}{T} \\ du &= c_V dT \quad R' = c_P - c_V \end{aligned}\right\} \tag{2}$$

being T the gas temperature, c_P and c_V the constant pressure and constant volume specific heat, and R' the gas constant.

The compression-expansion process in a motored engine can be assumed to be frictionless, hence the second law of thermodynamics states that the specific entropy variation dS of the in-cylinder gas is:

$$\mathrm{d}S = \frac{\mathrm{d}q}{T} \tag{3}$$

thus, from equations (1) and (2) the specific entropy variation results:

* Corresponding author. Tel.: +39 (0) 916657162; fax: +39 (0) 916657163.
E-mail address: pipitone@dima.unipa.it (E. Pipitone).

1359-4311/$ – see front matter © 2010 Elsevier Ltd. All rights reserved.
doi:10.1016/j.applthermaleng.2010.04.012

$$dS = \frac{du}{T} + \frac{p\,dv}{T} = c_V\frac{dT}{T} + R'\frac{dv}{v} = c_V\left(\frac{dp}{p} + \frac{dv}{v}\right) + (c_P - c_V)\frac{dv}{v} = c_V\frac{dp}{p} + c_P\frac{dv}{v} \tag{4}$$

Due to mass leakage through valve seats and piston rings, the available volume V for the in-cylinder gas increases, hence its specific volume changes:

$$V = v\cdot m \Rightarrow \frac{dv}{v} = \frac{dV}{V} - \frac{dm}{m} \tag{5}$$

where m represents the in-cylinder mass.

Hence, considering the finite increment "δ" due to a crank rotation $\delta\vartheta$, the specific entropy variation in equation (4) will now result:

$$\delta S = \frac{\delta q}{T} = c_P\frac{\delta V}{V} + c_V\frac{\delta p}{p} - c_P\frac{\delta m}{m} \tag{6}$$

being δm the mass entering the cylinder (which is negative whenever in-cylinder pressure is higher than outer pressure); from equation (6) the in-cylinder pressure changes then results:

$$\delta p = \frac{1}{V}[\delta Q(k-1) - kp\delta V] + kp\frac{\delta m}{m} \tag{7}$$

where $\delta Q = m\,\delta q$ represents the heat received by the gas (which is negative when the gas temperature is higher than wall temperature, i.e. $\delta Q \propto (T_{wall} - T)$) and $k = c_P/c_V$ is the isentropic coefficient.

In an ideal adiabatic motored engine both δQ and δm would be zero, and pressure would reach its maximum ($\delta p = 0$ in equation (7)) when the volume is minimum ($\delta V = 0$): the compression and the expansion strokes would cause in-cylinder pressure variations symmetric with respect to TDC and the Location of the Peak Pressure LPP (which can be easily determined with 0.1 precision by means of polynomial interpolation of the pressure curve sampled with 1 crank angle degrees resolution) would coincide with the position of the TDC. As is known, in a Temperature–Entropy (T, S) diagram the adiabatic compression-expansion process of the in-cylinder gas would be represented by two coincident segments (AB and BA in Fig. 1). If the compression-expansion process is diabatic (i.e. in presence of heat transfer), according to the second law of thermodynamics (equation (3)), the entropy variation depends on the gas temperature: when this is lower then wall temperature, heat transfer is positive and hence entropy increases; on the contrary, whenever gas temperature is above the wall temperature, entropy decreases. This explains the diabatic evolution reported both in Figs. 1 and 2: as can be observed, in adiabatic process, the maximum pressure condition is reached before the minimum volume, i.e. before the TDC. In a real motored engine, pressure variation is also influenced by mass leakage δm and, as shown by equation (7), together with heat transfer, it causes the pressure increase to be zero when the volume changes are still negative (i.e. during compression); hence these two phenomena cause the pressure curve to be asymmetric with respect to the TDC, shifting the LPP in advance with respect to the TDC position (as can also be seen from the pressure curve reported in Fig. 3, obtained by means of thermodynamic simulations performed using the model described in Appendix A): the angular distance between LPP and the TDC position is called "loss angle" (ϑ_{loss}), being related to the energy and mass losses, and usually assumes values between −0.4 and −1 CA degrees, depending on the entity of the heat transferred and the escaped mass:

$$\vartheta_{loss} = L_{PP} - L_{TDC} \tag{8}$$

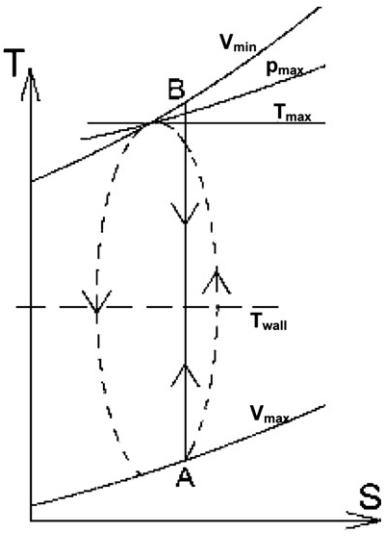

Fig. 1. Temperature–Entropy diagram of the compression-expansion process in a motored cylinder: ideal engine (segments AB and BA) and diabatic engine (dashed curve).

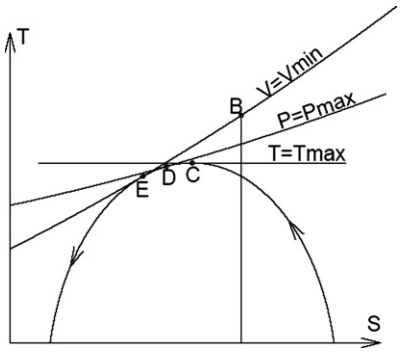

Fig. 2. Temperature–Entropy diagram of the diabatic compression-expansion process: peak pressure (point D) occurs before the TDC (point E).

1.1. The loss function and its increment

Equation (6) also shows that two easily measurable quantities, the in-cylinder pressure and volume, allow the evaluation of the entropy variation (i.e. heat transfer) together with the mass leakage by means of the functions $\delta V/V$ and $\delta p/p$, which are plotted as example in Fig. 5; defining the "*Loss function*" F so that:

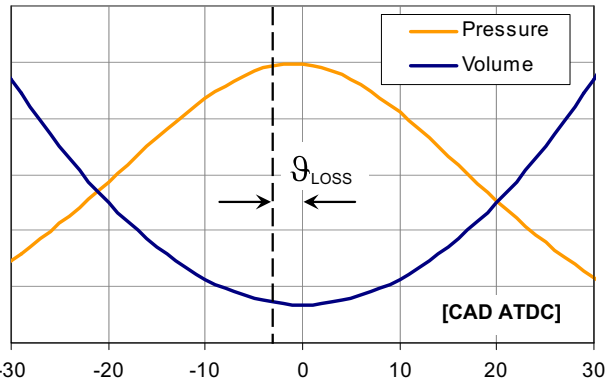

Fig. 3. Qualitative progress of in-cylinder pressure and volume near TDC.

$$\delta F = c_P \frac{\delta V}{V} + c_V \frac{\delta p}{p} \tag{9}$$

it will result:

$$\delta F = \delta S + c_P \frac{\delta m}{m} \tag{10}$$

The entity of the variation of the *Loss function*, δF, which gathers the sum of the two *losses*, is then determined by the capability of the cylinder walls to exchange heat with the gas and by the amount of gas escaping from the cylinder. The qualitative progress of the *Loss function* variation in a real cylinder during a compression-expansion process, together with its two constitutive terms δS and $c_P\ \delta m/m$, is shown for example in Fig. 4: the entropy variation starts with a positive value (being $T < T_{wall}$) and decreases, crossing the zero line when $T = T_{wall}$, and reaching a minimum near the TDC position (here the heat flux from the gas to the wall is maximum), then starts to increase becoming positive before the Bottom Dead Centre (BDC); the relative mass leakage $\delta m/m$, being related to the difference between in-cylinder pressure and outer pressure, follows a similar trend, reaching a minimum near the TDC: it follows that, in this position, the loss function variation equals the sum of the two loss angle causes. Following this concept the authors tried to obtain information on the loss angle entity directly from the loss function variation. When the gas pressure reaches the peak value (i.e.at LPP), the ratio $\delta p/p$ is zero, and equation (9) becomes:

$$\delta F_{LPP} = \left[c_P \frac{\delta V}{V}\right]_{LPP} \tag{11}$$

The latter equation shows that at the peak pressure position the knowledge of the loss function increment δF allows to determine the value of $\delta V/V$ which, depending only on engine geometry (see Fig. 5 and equation (12)), is a known function of the crank shaft position, and hence of the loss angle. The function $\delta V/V$ can be expressed as:

$$\frac{\delta V}{V} = \frac{\sin(\vartheta)\left(1 + \frac{\cos(\vartheta)}{\sqrt{\mu^2 - \sin^2(\vartheta)}}\right)\delta\vartheta}{\frac{2}{\rho - 1} + \mu + 1 - \cos(\vartheta) - \sqrt{\mu^2 - \sin^2(\vartheta)}} \tag{12}$$

where ρ is the volumetric compression ratio and μ expresses the rod to crank ratio (i.e. the ratio between connecting rod length and crank radius). Since the loss angle is normally around -1° ($= -0.017$ radians), further approximations can be made:

$$\sin(\vartheta_{loss}) \approx \vartheta_{loss} \quad \cos(\vartheta_{loss}) \approx 1$$

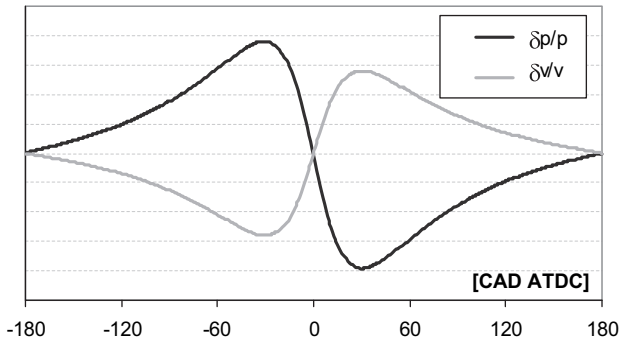

Fig. 5. Qualitative progress of $\delta V/V$ and $\delta p/p$ (obtained using the model described in Appendix A with $\delta\vartheta = 1$ CAD).

It follows that, at the peak pressure position, equation (12) becomes:

$$\left[\frac{1}{V}\frac{\delta V}{\delta\vartheta}\right]_{LPP} = \frac{\vartheta_{loss}\left(1 + \frac{1}{\sqrt{\mu^2 - \vartheta_{loss}}}\right)}{\frac{2}{\rho - 1} + \mu - \sqrt{\mu^2 - \vartheta_{loss}}} \tag{13}$$

Hence, being ${\vartheta_{loss}}^2 << \mu^2$, equations (11) and (13) yield:

$$\vartheta_{loss} = \frac{2}{\rho - 1} \cdot \frac{\mu}{\mu + 1} \cdot \left[\frac{1}{c_p}\frac{\delta F}{\delta\vartheta}\right]_{LPP} \tag{14}$$

This demonstrates that the loss angle can be easily correlated to the loss function increment δF evaluated at the peak pressure position. Unfortunately δF undergoes great distortions even with small phase errors between $\delta p/p$ and $\delta V/V$: Fig. 6, as example, shows some loss function variation curves calculated by means of the thermodynamic model exposed in Appendix A assuming different phase errors (expressed as fraction of the loss angle). As can be seen, a pressure phasing error equal to the loss angle (which means LPP = 0) introduces a considerable error in the evaluation of the function δF. This fact, without a reliable way to evaluate the δF at the peak pressure position, would make equation (14) useless. The same Fig. 6 however shows the existence of two zones common to each of the curves: in these two crank positions the two fundamental functions for the calculus of the entropy variation, $\delta p/p$ and $\delta V/V$, reach their extreme values (at about ±30 CAD ATDC in Fig. 5), and hence are poorly influenced by small phase errors (i.e. in the order of the loss angle); for this reason, according to equation (9), in these two crank positions the loss function variation remains almost unchanged. This fact implies that assuming a TDC position error equal to the loss angle (easily achievable setting LPP = 0), the values of the loss function variation δF_1 and δF_2 in the two points relative to

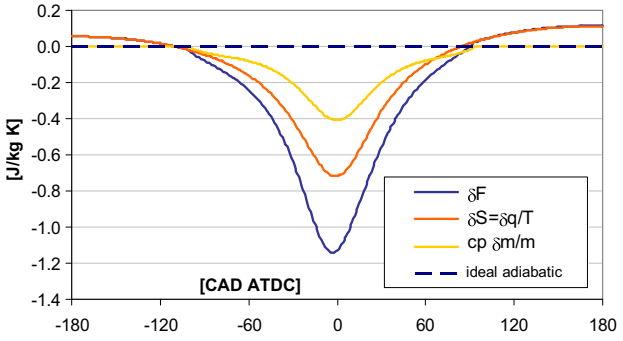

Fig. 4. Loss function variation δF and its two constitutive terms (obtained using the model described in Appendix A with $\delta\vartheta = 1$ CAD).

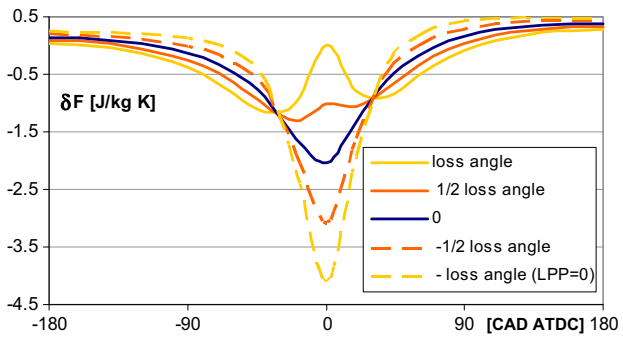

Fig. 6. Loss function variation δF for different phase errors (obtained using the model described in Appendix A with $\delta\vartheta = 1$ CAD).

the minimum and maximum of the function $\delta V/V$ will be nearly correct. Hence, in order to determine the loss angle from equation (14), a correlation between δF_1 and δF_{LPP} has been searched, and, as shown in Appendix B, it has been found that, for a given engine, the ratio between δF_{LPP} and δF_1 is almost constant, i.e.:

$$\delta F_{LPP} \approx \Phi \cdot \delta F_1 = \Phi \cdot \delta F_{\mathrm{mind}V/V} \quad (15)$$

where Φ is a proportionality constant.

As shown in Appendix B this constant mainly depends on the engine compression ratio and on the heat transfer law, and its mean value has been estimated to be 1.95. Thus equation (15) becomes:

$$\delta F_{LPP} \approx 1.95 \cdot \delta F_{\mathrm{mind}V/V} \quad (16)$$

As a result, the top dead centre position can be determined phasing the pressure cycle with an initial error equal to the loss angle (i.e. setting LPP = 0) and calculating the loss function increment δF_1 at the minimum $\delta V/V$ position ϑ_1, which requires, according to equation (9), the estimation of the functions $\delta V/V$ and $\delta p/p$. Unfortunately both of these functions can be affected by measurement errors: the in-cylinder pressure acquisition can be in fact subjected to bias error (above all if an un-cooled piezoelectric transducer is used) and to electric and mechanical noise, while the in-cylinder volume estimation may present inaccuracy related to the compression ratio, which is normally known with some approximation (±3%). Moreover, as shown in equation (9), the specific heat at constant pressure and volume are required, which are functions of the gas temperature; this in turn can be deduced applying the perfect gas law by means of the gas temperature at inlet valve closure, which is normally known with an approximation as high as 30 °C.

All these uncertainties may strongly affect the δF_1 evaluation, as shown for example in Fig. 7: here the loss function variation is calculated supposing both different compression ratio errors (top figure) and pressure bias errors (bottom figure). As can be seen, in presence of these measurement errors, the evaluated δF_1 may considerably differs from the real one (i.e. error = 0) thus preventing a reliable evaluation of the δF_{LPP} and hence of the loss angle.

However the same Fig. 7 also shows that the evaluated δF_1 and δF_2 move in different directions in consequence of the measurement errors: this effect implies their mean value δF_m remains almost constant, as shown in Table 1 and Table 2.

$$\delta F_m = \left(\frac{\delta F_1 + \delta F_2}{2}\right) = \left(\frac{\delta F_{\mathrm{mind}V/V} + \delta F_{\mathrm{maxd}V/V}}{2}\right) \quad (17)$$

It follows that, in order to correctly evaluate the loss angle, the loss function increment at the peak pressure position δF_{LPP} should be correlated with the mean value δF_m rather than with δF_1. Thus relations (15) becomes:

$$\delta F_{LPP} = \Phi \cdot \delta F_m \quad (18)$$

Therefore the method proposed by the authors reposes on the evaluation of loss function increment δF_1 and δF_2 at the minimum and maximum $\delta V/V$ positions (ϑ_1 and ϑ_2), which, according to equation (18), allows to evaluate the loss function variation at the peak pressure position δF_{LPP}; this, in turn, is linked to the loss angle ϑ_{loss} by means of equation (14) and furnishes the top dead centre position (see equation (8)). The determination of the angular positions ϑ_1 and ϑ_2 at which the function $\delta V/V$ is minimum and maximum requires the derivation of equation (12), whose result is a function not solvable in the variable ϑ.

Hence these angular positions must be evaluated using numeric methods; considering compression ratios ρ ranging from 10 to 20 and rod to crank ratios μ ranging from 2.8 to 4.0, the authors determined the angular positions ϑ_1 ($=-\vartheta_2$) using a 2nd order polynomial interpolation on the $\delta V/V$ curve extended to a range of ±0.4° around the position of the extreme values. The results, as pointed out in Fig. 8, showed that the angular positions ϑ_1 and ϑ_2 depend both on the compression ratio and on the rod to crank ratio. The data obtained allowed to trace a formula for the calculation of the minimum and maximum $\delta V/V$ angular positions with a precision of 0.1°:

$$\vartheta_{1,2} = \mp 76.307 \cdot \mu^{0.123} \cdot \rho^{-0.466} \quad [\mathrm{CAD\ ATDC}] \quad (19)$$

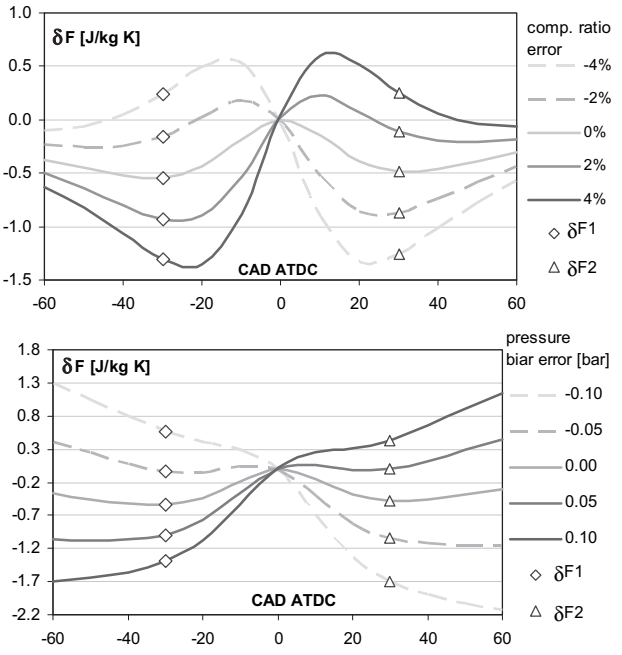

Fig. 7. Loss function variation δF in presence of compression ratio error (top) and pressure bias error (bottom): δF_1 (◇) and δF_2(△) are shown (pressure cycles phased with LPP = 0 obtained using the model described in Appendix A with $\delta\vartheta$ = 1 CAD).

Table 1
Percentage error on both δF_1 and δF_m for different pressure bias errors.

Pressure bias error [bar]	Err% δF_1	Err% δF_m
−0.15	−332%	18%
−0.10	−202%	11%
−0.05	−93%	5%
0.00	0%	0%
0.05	82%	−4%
0.10	155%	−8%
0.15	221%	−11%

Table 2
Percentage error on both δF_1 and δF_m for different compression ratio errors.

Compression ratio error	Err% δF_1	Err% δF_m
−6%	−219%	−3%
−4%	−144%	−2%
−2%	−71%	−1%
0%	0%	0%
2%	70%	1%
4%	138%	2%
6%	205%	3%

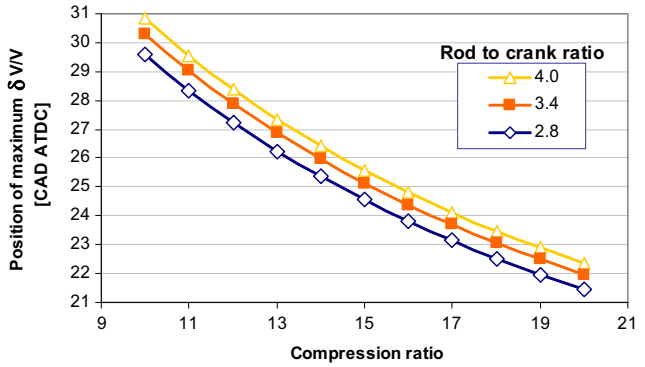

Fig. 8. Position of maximum $\delta V/V$ with varying compression ratio and for different rod to crank ratio.

1.2. Procedure for TDC position estimation

Summarizing, once the motored pressure cycle has been sampled, the procedure for the TDC estimation consist of 5 steps, here resumed:

1) the pressure cycle must be phased setting LPP = 0 (in this way the position error is exactly equal to the unknown loss angle ϑ_{loss}): for this purpose a 2nd order polynomial fitting performed on the pressure curve around the maximum pressure value position allows a sufficient precision
2) the angular position ϑ_1 and ϑ_2 of the minimum and maximum $\delta V/V$ must be evaluated (for example using equation (19))
3) the loss function increments δF_1 and δF_2 at the angular position ϑ_1 and ϑ_2 must be calculated by means of equation (9)

$$\delta F = c_P \frac{\delta V}{V} + c_V \frac{\delta p}{p}$$

and hence their mean value $\delta F_m = 1/2\ (\delta F_1 + \delta F_2)$

4) the loss function increment δF_{LPP} at the peak pressure position can be determined from equation (18)

$$\delta F_{LPP} = \Phi \cdot \delta F_m$$

where the constant Φ can be estimated by means of equation (46) (reported Appendix B) or set to the mean value 1.95, as determined in Appendix B

5) the loss angle ϑ_{loss}, and hence the TDC location, can be then evaluated by means of equation (14)

$$\vartheta_{loss} = \frac{2}{\rho - 1} \cdot \frac{\mu}{\mu + 1} \cdot \left[\frac{1}{c_p} \frac{\delta F}{\delta \vartheta} \right]_{LPP}$$

It is worthwhile to mention that the first step is not necessary if the pressure cycle has already been phased with an error lower than the loss angle. Moreover the specific heat c_P and c_V in equations (6), (9), (11) and (14) should be temperature dependent and evaluated according to the classical known functions valid for air, as reported in Appendix A. However a satisfactory approximation is equally reached if the c_P and c_V are supposed to be constant. In this case the evaluation of the gas temperature is completely avoidable for the TDC determination.

2. Assessment of the method

In order to ascertain the reliability of the method proposed, a series of simulations has been performed to generate plausible in-cylinder pressure curves compatible with the real compression-expansion process which takes place in a motored engine cylinder, taking into account both mass leakages and heat transfers. The pressure curves obtained have been then used to test both the reliability of the proposed method in the determination of TDC and its robustness to the most common encountered measurement problems. Details on the thermodynamic model used for the generation of the pressure curves are given in Appendix A.

A first series of simulations has been performed in order to estimate the entity of the loss angle and its dependence from the engine operative condition of speed and Manifold Absolute Pressure (MAP). The simulations were carried out, as resumed in Table 3, taking into consideration the dimensions of a commercial available automotive engine, two compression ratios (10 and 22), different conditions of MAP and speed and employing three different heat transfer models (reported in Appendix A). For each simulated pressure curve, the seven points around the maximum value have been interpolated by means of a 2nd order polynomial, thus obtaining the location of the pressure peak (LPP) as the vertex abscissa: this procedure ensured a precision of 0.001 CAD, which is amply higher than the required one of 0.1 CAD. Once known the LPP, the loss angle is known by its definition:

$$\vartheta_{loss} = L_{PP} - L_{TDC}$$

As a result, the diagrams in Fig. 9 shows the loss angle values obtained with compression ratio = 10 employing the Woschni heat

Table 3
Simulation conditions for the evaluation of the loss angle entity (more details can be found in Appendix A).

Manifold absolute pressure	0.4 to 1.0 bar (steps of 0.1)
Engine speed	1000 to 3000 rpm (steps of 500)
Compression ratio	10 and 22
Rod to crank ratio	3.27
Bore	70.80 mm
Stroke	78.86
Leakage flow area A_N	0.507 mm^2
Walls temperature	70 °C

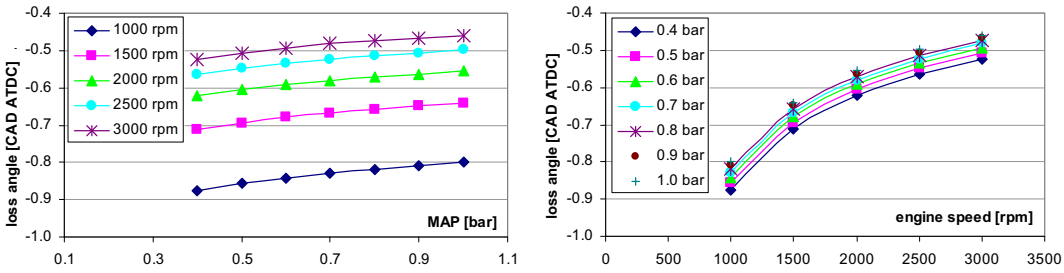

Fig. 9. Loss angle value determined with compression ratio $\rho = 10$ using the Woschni heat transfer model.

Table 4
Loss angle values determined with low compression ratio.

Comp. ratio = 10			
Heat transf. model	Woschni	Eichelberg	Hoenberg
Loss angle	−0.62	−0.64	−0.85
Variation range	±0.21	±0.36	±0.31

Table 5
Loss angle values determined with high compression ratio.

Comp. ratio = 22			
heat transf. model	Woschni	Eichelberg	Hoenberg
loss angle	−0.63	−0.62	−0.88
variation range	±0.22	±0.34	±0.31

transfer model. It can be observed that the loss angle, whose values go from −0.46 to −0.88, mainly depends on engine speed, while the manifold pressure plays a minor role. Since the two causes of the loss angle, heat transfer and mass leakage, decrease their entities with growing engine speed, then the loss angle diminishes too. The manifold pressure influences both the relative mass leakage $\delta m/m$ and the specific heat exchanged with walls, causing then lower loss angles with higher MAP. The mean loss angle values estimated both for low and high compression ratio engines according to each of the three heat transfer models are resumed in Table 4 and Table 5, together with their variation ranges. As shown, there are no great differences between the two compression ratios: using the Woschni and the Eichelberg models, the loss angle resulted to be about −0.63 CAD, while employing the Hoenberg model, the mean loss angle was found to be about −0.87 CAD. This different prediction is due to the higher heat exchange coefficient which characterize the Hoenberg model with respect to the other two (see Fig. 10 and Fig. 11).

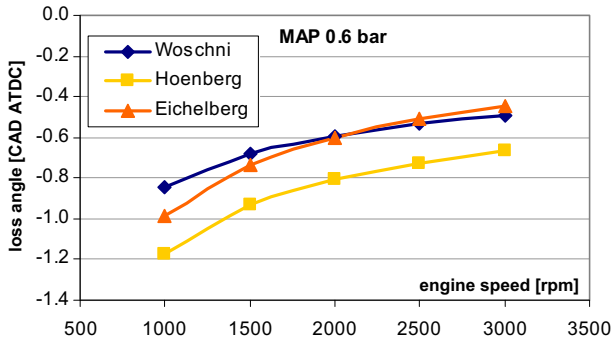

Fig. 10. Comparison between the loss angle values determined at MAP = 0.6 bar using the three heat transfer models (engine with $\rho = 10$).

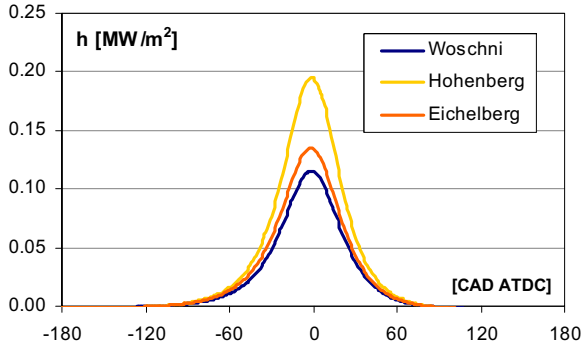

Fig. 11. Heat exchange coefficients according to the three heat transfer models at 1500 rpm and MAP = 0.6 bar (engine with $\rho = 10$).

2.1. Application of the method proposed

The application of the proposed method requires the calculation of the loss function increment δF at the angular position ϑ_1 and ϑ_2 (see equation (19)) relative to the minimum and maximum $\delta V/V$; in these two positions both $\delta V/V$ and $\delta p/p$ must be evaluated (see equation (6)), together with the gas temperature, which allows the determination of both c_P and c_V (see equation (32) in Appendix A). The relative volume change $\delta V/V$ can be easily estimated, since the engine dimensions are generally known; hence, as already shown in equation (12):

$$\frac{\delta V}{V} = \frac{\sin(\vartheta)\left(1 + \frac{\cos(\vartheta)}{\sqrt{\mu^2 - \sin^2(\vartheta)}}\right)\delta\vartheta}{\frac{2}{\rho - 1} + \mu + 1 - \cos(\vartheta) - \sqrt{\mu^2 - \sin^2(\vartheta)}}$$

where ϑ represents the crank angular position ($\vartheta = 0$ at TDC). It must be pointed out that this expression is valid for a centred crank mechanism: the case of a non centred crank mechanism is discussed below.

The evaluation of the relative pressure change $\delta p/p$ may presents, instead, some problems related to the in-cylinder pressure acquisition, which is generally performed with one crank angle degree resolution. The authors propose the following procedure for the calculation of $\delta p/p$ at ϑ_1 and ϑ_2: first of all the relative pressure increment must be numerically evaluated, hence:

$$\left(\frac{\delta p}{p}\right)_i = \frac{(p_{i+1} - p_{i-1})}{2p_i} \tag{20}$$

Then the $\delta p/p$ values must be interpolated, as function of the crank position, by means of a 3rd degree polynomial (which revealed to give better results than the 2nd and the 4th order polynomial) in the range of ±20° around ϑ_1 and ϑ_2; the fitting polynomials thus obtained permit the precise evaluation of $\delta p/p$ at ϑ_1 and ϑ_2 position. As pointed out below, this procedure is also useful for noise filtering purpose.

The first series of simulations aimed to verify, both for a constant mass process and in presence of gas leakage, the value of the proportionality constant Φ calculated in the Part 1. To that end the pressure curves have been computed according to each of the three heat transfer models with and without mass leakage, for different manifold pressure and engine speed conditions, and assuming various compression ratio and rod to crank ratio (i.e. the ratio between connecting rod length and crank radius), thus generating 1050 different pressure cycles, as summarized in Table 6.

For each of the simulated pressure cycles, the above resumed 5-steps procedure has been applied in order to evaluate the loss

Table 6
Simulation conditions for the evaluation of the proportionality constant Φ.

Manifold absolute pressure	0.4 to 1.0 bar (steps of 0.1)
Engine speed	1000 to 3000 rpm (steps of 500)
Compression ratio	10 to 20 (steps of 2)
Rod to crank ratio	2.8 to 4.0 (steps of 0.3)
Bore	70.8 mm
Bore to stroke ratio	1
Leakage flow area	0.507 mm^2
Walls temperature	70 °C

angle value, which in turn allows to estimate the TDC location: this, compared to the known TDC location of the thermodynamic model, allowed to determine the TDC estimation error of the method proposed for each of the pressure cycles.

The results obtained confirmed the evaluation carried out in Appendix B: in fact the top diagram in Fig. 12, which reports the maximum error in the TDC position evaluation for a constant mass process and for each of the heat transfers models, shows that $\Phi = 1.92$ provides the best compromise between the different heat transfer models. When also the effect of gas leakages is considered, as predicted in Appendix B, the proportionality constant tends to increase, as confirmed by the bottom diagram in Fig. 12: in this case in fact a safer value would lie between 1.95 and 2, minimizing thus the loss angle evaluation error. It is worthwhile to mention that this result however depends on the gas leakage entity, i.e. on the value adopted for the equivalent flow area (see Appendix A for more details). The diagrams in Fig. 12 also show that in both cases the entity of the error committed on the loss angle value is safely below the allowable 0.1 CAD: this result confirms the validity of the method proposed for the determination of the top dead centre position.

2.2. Assessment of the method's robustness

Once confirmed the validity of the method proposed, the authors assessed its robustness towards the most common in-cylinder pressure measurement problems and uncertainties, which are here listed:

1) Pressure bias error: this kind of error is typical when dynamic sensors or sensors subjected to thermal drift (e.g. an un-cooled piezoelectric sensors) are employed. If the measured pressure cycle is compensated by means of one of the most known methods [10,11], the pressure evaluation uncertainties may be as high as 10 kPa: the effect of such a measurement error on the loss function increment δF has already been shown in Fig. 7 and Table 1.
2) Engine compression ratio: this fundamental parameter is normally known with some approximation, typically ±3%. Such uncertainty may introduce an estimation error on the evaluation of in-cylinder volume, which in turn may affect the reliability of the method proposed, which relies on the function $\delta V/V$; Fig. 7 and Table 2 show the effect of a ±4% compression ratio error on the estimation of the loss function increment δF.
3) In-cylinder gas temperature: during the compression-expansion process it can be evaluated by means of the perfect gas law, on the base of the gas temperature at inlet valve closure T_{IVC}, which, taking into account wall heat transfer during the intake stroke, is usually assumed to be 15÷30 °C higher than the manifold gas temperature. This estimation may introduce an error as high as ±30 °C.
4) Pressure measurement noise: it is known to internal combustion engine researchers that a noise component is always present in the pressure signal measured. It may origin from the mechanical vibrations perceived by the transducer or from electromagnetic interferences. Analysing some experimental pressure cycles sampled on a spark ignition engine, it was found that the intensity of such a noise typically reaches a 600 Pa standard deviation. Fig. 13 shows the strong effect on the loss function increment δF of a uniform noise with a standard deviation of 400 Pa.

The dimensions of the engine considered in the robustness were the same of Table 3. The compression-expansion process has been simulated by means of the thermodynamic model described in Appendix A on different conditions of engine speed and MAP (35 operative points), as summarized in Table 7.

For these simulations, just the Woschni heat transfer model was employed (which is the only one developed both on motored and fired engine cycles [7]) since the attention was focused on the robustness of the methods. The pressure curves obtained by the simulations were modified introducing the above mentioned measurement errors, as described in the following equations:

$$\begin{aligned} p' &= p + p_{bias} + p_{noise} \\ T_{IVC}' &= T_{IVC} + error_T \\ \rho' &= \rho \cdot (1 + error_\rho) \end{aligned} \quad (21)$$

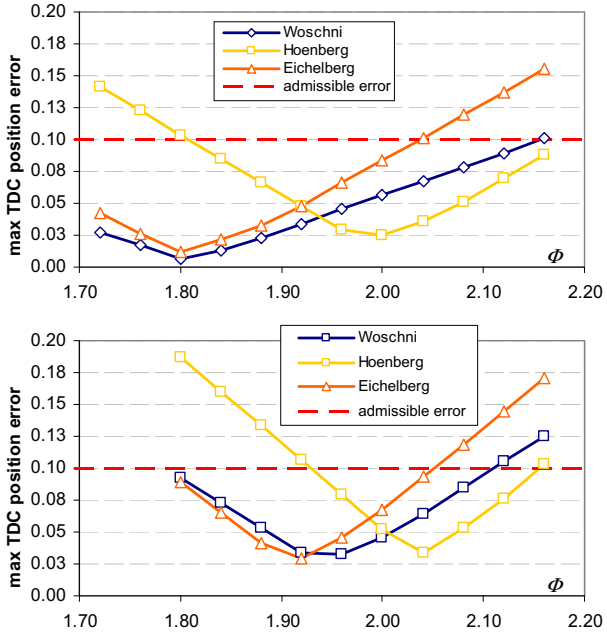

Fig. 12. Maximum TDC position error as function of the proportionality constant Φ: heat transfer only (top), both heat transfer and mass leakage (bottom).

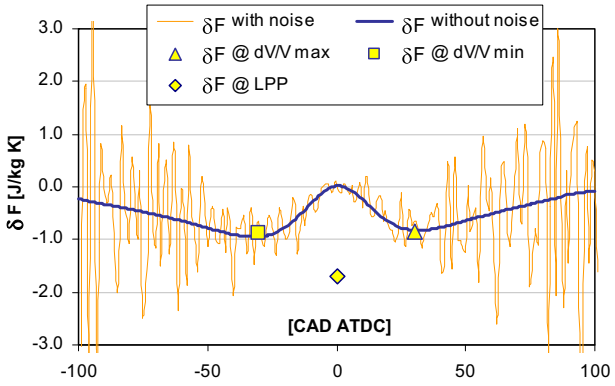

Fig. 13. Loss function increment δF with and without a 400 Pa standard deviation noise disturb ($\rho = 10$, pressure cycle phased with LPP = 0).

Table 7
Simulation conditions for the robustness tests.

Manifold absolute pressure	0.4 to 1.0 bar (step = 0.1)
Engine speed	1000 to 3000 rpm (step = 500)
T_{IVC}	35 °C
T_{wall}	70 °C

Table 8
Maximum TDC position errors for different measurement disturbances – ($\rho = 10$, $\Phi = 1.95$).

	Disturbance entity	Max TDC position error [CAD]
No disturbance		0.042
T_{IVC}	+30 °C	0.041
T_{IVC}	−30 °C	0.044
Compression ratio	+5%	0.045
Compression ratio	−5%	0.038
Pressure bias error	+10 kPa	0.034
Pressure bias error	−10 kPa	0.063
Pressure signal noise	st. dev. 600 Pa	0.043

On a first step the measurement errors were introduced one at a time, then the resulting pressure, volume and temperature data were employed to compute the loss angle by means of the proposed method. Table 8 reports the maximum TDC position error found for each of the disturbances introduced: as can be seen, it remained always below the 0.1°. The worst effect is played by the negative pressure bias error, while noise effect was adequately attenuated by means of the filtering properties of the 3rd order polynomial used to fit the $\delta p/p$ values.

In order to test the robustness of the method also for a high compression ratio engine, the simulations of Table 7 have been repeated setting the compression ratio to 22. Each disturbance has been applied again identically, except for the noise, which has been supposed to increase proportionally to the pressure levels, and has been amplified to reach a standard deviation of 1800 Pa. As shown in Table 9 the results obtained confirmed the reliability of the method even with high compression ratio engine, safely reaching the required precision of 0.1 CAD.

Even if the method proposed revealed to be robust against each of the measurement errors assumed, it must be considered that in a real experimental test these disturbances may occur simultaneously. Hence, in order to assess the robustness of the method when the disturbances are simultaneously present, the pressure cycles simulated in the 35 operative conditions of Table 7 were modified using the combination of disturbances reported in Table 10 and then employed to determine the loss angle by means of the proposed method. The maximum TDC position errors obtained for each disturbances combination are presented in Table 11 both for low and high compression ratio: as shown, in the case of low compression ratio ($\rho = 10$), the simultaneous presence of disturbances induced a maximum errors of 0.066 CAD, while in the case of high compression ratio engine ($\rho = 22$), the maximum TDC position evaluation error was 0.048 CAD.

The method proposed hence revealed to be robust enough to allow a safe evaluation of the TDC position (the maximum error was lower than the required 0.1 crank angle degrees) even in presence of the typical in-cylinder pressure measurement errors and disturbances.

Table 9
Maximum TDC position errors for different measurement disturbances – ($\rho = 22$, $\Phi = 1.95$).

	Disturbance entity	Max TDC position error [CAD]
No disturbance		0.048
T_{IVC}	+30 °C	0.050
T_{IVC}	−30 °C	0.048
Compression ratio	+5%	0.050
Compression ratio	−5%	0.047
Pressure bias error	+10 kPa	0.045
Pressure bias error	−10 kPa	0.05
Pressure signal noise	st. dev. 1800 Pa	0.041

Table 10
Disturbances combinations used in the robustness test.

Pressure signal noise	st. dev. 600 Pa ($\rho = 10$) or 1800 Pa ($\rho = 22$)							
T_{IVC} error	−30 °C				+30 °C			
Compression ratio error	−5%		+5%		−5%		+5%	
Pressure bias error [kPa]	−10	+10	−10	+10	−10	+10	−10	+10

Table 11
Maximum TDC position error obtained in the robustness test of Table 10.

	Maximum TDC position errors [CAD]							
compression ratio = 10	0.058	0.035	0.065	0.039	0.061	0.032	0.066	0.036
compression ratio = 22	0.041	0.037	0.045	0.041	0.045	0.037	0.048	0.040

2.3. Non centred crank mechanism

If the engine is endowed of a non centred crank mechanism, the crank angle position with respect to the cylinder axis when the connecting rod and the crank are aligned (i.e. when the piston is at top dead centre) is not zero but assumes the value ϑ_T, as depicted in Fig. 14.

If the angular position are still evaluated with respect to the cylinder axis, then the angle ϑ_T must be accounted for in order to correctly evaluate the TDC position by means of the thermodynamic method. As shown in Fig. 14, the angular positions of Top (ϑ_T) and Bottom (ϑ_B) Dead Centre can be calculated since:

$$\sin\vartheta_T = \frac{z}{l+r} \quad \sin\vartheta_B = \frac{z}{l-r} \tag{22}$$

where z is the crank pin offset (i.e. the distance between the crank pin and the cylinder axis), while l and r are the connecting rod length and the crank radius respectively. For a non centred crank mechanism, the piston stroke results to be:

$$c = \sqrt{(l+r)^2 - z^2} - \sqrt{(l-r)^2 - z^2} \tag{23}$$

hence, from Fig. 14, the in-cylinder volume is:

$$V = A_C \cdot \left[\frac{c}{\rho - 1} + (l+r)\cdot\cos\vartheta_T - l\sqrt{1 - \left(\tau - \frac{\sin\vartheta}{\mu}\right)^2} - r\cdot\cos\vartheta \right] \tag{24}$$

being A_C the cylinder section area and τ the ratio z/l.

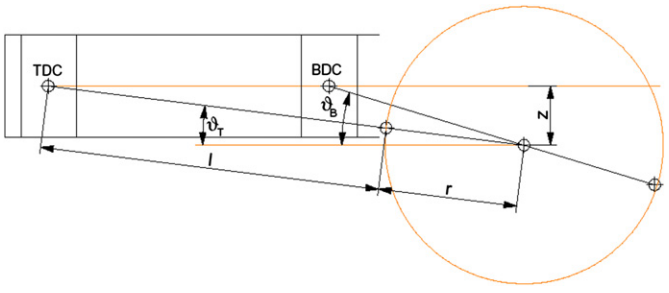

Fig. 14. Representation of a non centred crank mechanism.

Equation (12) then becomes:

$$\frac{\delta V}{V}=\frac{\sin\vartheta\cdot\left(1+\frac{\cos\vartheta-\tau\mu\cdot\cot\vartheta}{\sqrt{\mu^2-(\sin\vartheta-\tau\mu)^2}}\right)}{\frac{c}{r\cdot(\rho-1)}+(\mu+1)\cdot\cos\vartheta_T-\mu\cdot\sqrt{1-\left(\tau-\frac{\sin\vartheta}{\mu}\right)^2}-\cos\vartheta}\cdot\delta\vartheta \quad (25)$$

which, besides allowing the correct estimation of the loss function increment δF by means of equation (6), can also be used for the numerical evaluation of the angular position ϑ_1 and ϑ_2 of minimum and maximum $\delta V/V$ through polynomial interpolation: the authors however observed that, for this purpose, equation (19), which has been derived for centred crank mechanism, still gives good results. Being the loss angle in the order of -1 CAD ≈ -0.017 radians, the following approximation can be made:

$$\begin{aligned}&\vartheta_{loss}<<1\Rightarrow\sin\vartheta_{loss}\approx\vartheta_{loss}\quad\cos\vartheta_{loss}\approx1\\&\left(\tau-\tfrac{\sin\vartheta_{loss}}{\mu}\right)^2<<1\Rightarrow\sqrt{1-\left(\tau-\tfrac{\sin\vartheta_{loss}}{\mu}\right)^2}\approx1\end{aligned} \quad (26)$$

hence equation (25) becomes:

$$\left[\frac{\delta V}{V}\right]_{\mathrm{LPP}}=\frac{\vartheta_{\mathrm{loss}}+\frac{\vartheta_{\mathrm{loss}}}{\mu}-\tau}{\frac{c}{r\cdot(\rho-1)}+(\mu+1)\cdot\cos\vartheta_{\mathrm{T}}-\mu-1}\cdot\delta\vartheta \quad (27)$$

The crank pin offset z is usually small with respect to the rod length l, then also $\vartheta_{\mathrm{T}}<<1$ and hence.

$$\cos\vartheta_{\mathrm{T}}\approx1\quad\vartheta_{\mathrm{T}}\approx\sin\vartheta_{\mathrm{T}}=\frac{z}{l+r}=\frac{\tau}{1+1/\mu}=\frac{\mu\cdot\tau}{\mu+1} \quad (28)$$

Equation (27) thus gives:

$$\left[\frac{\delta V}{V}\right]_{\mathrm{LPP}}=\frac{\vartheta_{\mathrm{loss}}\cdot\left(\frac{1+\mu}{\mu}\right)-\tau}{\frac{c}{r\cdot(\rho-1)}}\cdot\delta\vartheta \quad (29)$$

which, together with the latter of equations (28) and equation (11), allows to evaluate the loss angle:

$$\begin{aligned}\vartheta_{\mathrm{loss}}&=\frac{\tau\cdot\mu}{\mu+1}+\frac{c/r}{\rho-1}\cdot\frac{\mu}{\mu+1}\cdot\left[\frac{1}{c_{\mathrm{p}}}\frac{\delta F}{\delta\vartheta}\right]_{\mathrm{LPP}}\\&=\vartheta_T+\frac{c/r}{\rho-1}\cdot\frac{\mu}{\mu+1}\cdot\left[\frac{1}{c_{\mathrm{p}}}\frac{\delta F}{\delta\vartheta}\right]_{\mathrm{LPP}}\end{aligned} \quad (30)$$

As can be noted equation (30) differs from equation (14) for the presence of the angular offset ϑ_{T} and for the ratio c/r which is less than 2 for a non centred crank mechanism.

In order to verify the reliability of the method with a non centred crank mechanism, the simulations in the operative conditions of Table 7 have been repeated with and without measurement disturbances using the engine data of Table 12: the results, resumed in Table 13, clearly show that the method proposed still estimates the TDC position with a maximum error of 0.049 CAD.

Table 14 instead reports the maximum TDC position estimation errors obtained with the simultaneous presence of the measurement disturbances for each of the 35 operative conditions: also in this case the maximum TDC position errors found remained under the required accuracy of 0.1 CAD. The method proposed thus revealed a good reliability even when the engine used is characterized by a non centred crank mechanism.

Table 12
Dimensions of the engine with crank pin offset.

Compression ratio	10
Rod to crank ratio	3.27
Bore	70.80 mm
Crank radius	35.40 mm
Crank pin offset	2 mm ($\tau=0.017$)
Leakage flow area	0.507 mm^2

Table 13
Maximum TDC position errors for different measurement disturbances (non centred crank mechanism, $\Phi=1.95$).

	Disturbance entity	Max TDC position error [CAD]
No disturbance		0.015
T_{IVC}	+30 °C	0.014
T_{IVC}	−30 °C	0.024
Compression ratio	+5%	0.018
Compression ratio	−5%	0.018
Pressure bias error	+10 kPa	0.032
Pressure bias error	−10 kPa	0.039
Pressure signal noise	st. dev. 600 Pa	0.049

3. Conclusions

As is known to internal combustion engines researcher, the exact determination of the crank position when the piston is at Top Dead Centre (TDC) is of crucial importance for indicating analysis: the maximum allowable error results to be about 0.1 Crank Angle Degrees (CAD). Due to wall heat transfer and mass leakage, under motored condition (i.e. without combustion) the TDC position does not coincide with the Location of Pressure Peak (LPP) but follows it by an angular arc called "*loss angle*", which, depending on the engine, is normally in the range of 1 Crank Angle Degrees (CAD).

This paper presents a new thermodynamic method for the estimation of the TDC position in internal combustion engines. The method relies on the definition of a proper function, called "*loss function*" whose increment is directly connected to the two "*losses*", i.e. wall heat transfer and gas leakage.

As described in the first part of the paper, the estimation of the *loos function* increment in two particular crank positions allows to determine the loss angle.

In the second part of the paper, the method is put to the test by means of thermodynamic simulations, thus verifying its capability to determine the loss angle under many different operative conditions of engine speed and manifold pressure, both for low and high compression ratio engines, and using three different heat release models. Moreover, typical in-cylinder pressure measurement errors and disturbances (pressure bias errors, pressure signal noise, compression ratio and gas temperature uncertainty) have

Table 14
Maximum TDC position errors obtained in the robustness test (non centred crank mechanism, $\Phi=1.95$).

Pressure signal noise	st. dev. 600 Pa							
T_{IVC} error	−30 °C				+30 °C			
Compression ratio error	−5%		+5%		−5%		+5%	
Pressure bias error [kPa]	−10	+10	−10	+10	−10	+10	−10	+10
Max TDC position error	0.044	0.058	0.044	0.058	0.045	0.073	0.045	0.073

been taken into account in order to test the robustness of the method proposed: as a result, the proposed thermodynamic method revealed a very good accuracy and reliability in determining the TDC position, assuring the required accuracy of 0.1 CAD even in presence of considerable disturbances, both for centred and non centred crank mechanism.

It is worthwhile to mention that the method proposed is intrinsically robust towards the entity of both heat transfer and mass leakage because it "weighs up" the effect of both "losses" in two particular crank positions and then estimates the entity of the two "losses" at the peak pressure position, which in turn allows to evaluate the loss angle. This means that the method proposed maintain its precision apart from the amount of both heat exchanged with wall and mass escaped from the cylinder.

Appendix A. Thermodynamic model used for the simulation of the compression-expansion process in a motored engine cylinder

This section gives some details on the thermodynamic model used for the compression-expansion process simulation.

The model employed is zero dimensional and has been implemented on a spreadsheet with a resolution of 1 crank angle degree. It is based on the first law of thermodynamics, which allows to calculate the pressure variation of the gas (air) due to in-cylinder volume changes during both the compression and expansion strokes. As already described above, equations (1)–(6) allow the estimation of the in-cylinder pressure variation during a crank rotation $\delta\vartheta$:

$$\delta p = \frac{1}{V}[\delta Q(k-1) - kp\delta V] + kp\frac{\delta m}{m} \tag{31}$$

where V represents the in-cylinder volume, p the gas pressure, δQ the heat received by the gas from the cylinder walls, $k = c_P/c_V$ is the isentropic coefficient, m represents the in-cylinder mass while δm is the mass entering the cylinder (hence for mass leakage δm is negative).

In the thermodynamic model both c_P and c_V were considered function of the gas temperature by means of the equations valid for Air:

$$c_P = 1403.06 - 360.72\left(\frac{1000}{T}\right) + 108.24\left(\frac{1000}{T}\right)^2 - 10.79\left(\frac{1000}{T}\right)^3 \quad [\mathrm{J/kgK}] \tag{32}$$

$$c_V = c_P - R' \quad \text{and} \quad R' = 287.1 \ [\mathrm{J/kgK}] \quad k = c_P/c_V$$

As regards wall heat transfers, three different models have been considered, in order to assess the results of the method independently from the heat exchange law:

a) Woschni model [7,8] $h = 3.26\cdot d^{-0.2}\cdot(2.28\cdot u_m)^{0.8}\cdot T^{-0.53}\cdot p^{0.8}$ $[\mathrm{W/m^2K}]$

where, d = cylinder bore [m], T = gas temperature [K], p = gas pressure [kPa], u_m = mean piston speed [m/s].

b) Hoenberg model [7] $h = 130\cdot V^{-0.06}(u_m + 1.4)^{0.8}\cdot T^{-0.4}\cdot p^{0.8}$ $[\mathrm{W/m^2K}]$

where, V = instantaneous cylinder volume [m3], T = gas temperature [K], p = gas pressure [bar], u_m = mean piston speed [m/s].

c) Eichelberg model [7,9] $h = 2.43\cdot u_m 0.33\cdot(p\cdot T)^{0.5}$ $[\mathrm{W/m^2K}]$

where, T = gas temperature [K], p = gas pressure [bar], u_m = mean piston speed [m/s].

It is worth to mention that in the above listed heat transfer models, any term related to the combustion pressure has been omitted, since the task is to simulate the pressure changes in a motored (i.e. without combustion) engine. Once fixed the model, the heat received by the gas during the interval time δt (i.e. in the rotation arc $\delta\vartheta$) can be evaluated as:

$$\delta Q = h\cdot \Delta T\cdot A\cdot \delta t = \frac{h\cdot \Delta T\cdot A\cdot \delta\vartheta}{\omega}$$

being ω the engine speed [rad/sec], $\Delta T = T_{wall} - T$ the temperature difference between cylinder walls and gas, and A the instantaneous in-cylinder walls surface.

Gas leakage has been modelled as the mass flowing through an equivalent convergent nozzle, hence the mass δm entered in the time interval δt can be evaluated as:

$$\delta m = -G_{nozzle}\cdot\delta t = \frac{-G_{nozzle}\cdot\delta\vartheta}{\omega} \tag{33}$$

where the mass flow G_{nozzle} naturally depends on the in-cylinder condition of pressure and temperature, and on the expansion ratio p_{out}/p:

$$G_{nozzle} = \begin{cases} A_N\sqrt{\dfrac{2k}{k-1}\,m\,\dfrac{p}{V}\left[\left(\dfrac{p_{out}}{p}\right)^{\frac{2}{k}} - \left(\dfrac{p_{out}}{p}\right)^{\frac{k+1}{k}}\right]} & \text{if } \dfrac{p_{out}}{p} > \left[\dfrac{p_{out}}{p}\right]_{CR} \approx 0.53 \\ A_N\sqrt{k\,m\,\dfrac{p}{V}\left(\dfrac{2}{k+1}\right)^{\frac{k+1}{k-1}}} & \text{if } \dfrac{p_{out}}{p} \le \left[\dfrac{p_{out}}{p}\right]_{CR} \approx 0.53 \end{cases} \tag{34}$$

Here A_N represents the equivalent nozzle flow area, which has been estimated by means of the results exposed in [5] keeping a constant proportionality with the piston surface area (see Table 6 and Table 12).

The crank rotation taken into consideration in the simulation ranged from −180 to +180 CAD after top dead centre (ATDC), with neither inlet valve lag angle nor advanced opening of the exhaust valve.

The pressure increment of equation (31) has been numerically integrated using the Runge-Kutta fourth order method thus

obtaining the in-cylinder pressure; the gas temperature has been calculated by means of the perfect gas law:

$$T = \frac{p}{p_{IVC}}\frac{V}{V_{IVC}}T_{IVC} \tag{35}$$

where p_{IVC}, V_{IVC} and T_{IVC} denote the thermodynamic state of the gas at the inlet valve closure.

Appendix B

In this section an analytical relation between the loss function variation at the peak pressure position δF_{LPP} and at the minimum $\delta V/V$ position δF_1 is derived.

As first step, the in-cylinder evolution will be considered without mass leakage; hence the ratio between the two loss function increments can be expressed in terms of entropy variations:

$$\frac{\delta F_{LPP}}{\delta F_{\vartheta_1}} \equiv \frac{\delta S_{LPP}}{\delta S_{\vartheta_1}} = \frac{[\delta Q/T]_{LPP}}{[\delta Q/T]_{\vartheta_1}} \tag{36}$$

where the amount of heat received by the gas from the walls during the time interval δt is:

$$\delta Q = hA(T_{wall} - T)\delta t \tag{37}$$

being h the heat transfer coefficient, A the area of the heat exchange surface, T and T_{wall} the gas and wall temperatures. Hence the entropy variations ratio becomes:

$$\frac{\delta S_{LPP}}{\delta S_{\vartheta_1}} = \frac{[hA(T_{wall} - T)/T]_{LPP}}{[hA(T_{wall} - T)/T]_{\vartheta_1}} \tag{38}$$

The total in-cylinder wall surface area A is:

$$A = \pi \cdot d \cdot \left(x + \frac{d}{2}\right) = \frac{\pi \cdot d^2}{2}\left(\frac{x}{d/2} + 1\right) \tag{39}$$

where x represents the piston distance from the cylinder top (function of the crank angle ϑ):

$$x = \frac{d}{2}\left[\frac{2}{\rho - 1} + 1 - \cos(\vartheta) + \frac{sen(\vartheta)^2}{2\mu}\right] \tag{40}$$

Here ρ is the volumetric compression ratio, while μ is the rod to crank ratio (i.e. the ratio between the connecting rod length and the crank radius). Introducing the dimensionless variable $\chi = 2x/d$, the ratio between the heat transfer surfaces become:

$$\frac{A_{LPP}}{A_{\vartheta_1}} = \frac{[\chi + 1]_{LPP}}{[\chi + 1]_{\vartheta_1}} \tag{41}$$

According to the most used model for heat transfer between gas and internal combustion engine cylinder, the heat transfer h coefficient is related to gas pressure p, temperature T and volume V by means of three power with exponents a, b and c respectively:

$$h \ \alpha \ p^a T^b V^c$$

Hence the ratio of the heat transfer coefficient becomes:

$$\frac{h_{LPP}}{h_{\vartheta_1}} = \frac{\left[p^a T^b V^c\right]_{LPP}}{\left[p^a T^b V^c\right]_{\vartheta_1}} \tag{42}$$

Both gas pressure and temperature are linked to in-cylinder volume by the polytropic law:

$$pV^\gamma = cost$$
$$TV^{\gamma-1} = cost$$

where γ is the mean polytropic index.

It follows that the ratio between the heat transfer coefficient is:

$$\frac{h_{LPP}}{h_{\vartheta_1}} = \left(\frac{V_{\vartheta_1}}{V_{LPP}}\right)^{\gamma(a+b)-b-c} = \left(\frac{\chi_{\vartheta_1}}{\chi_{LPP}}\right)^{\gamma(a+b)-b-c} \tag{43}$$

The last fundamental ratio in equation (38) regards the temperature difference between gas and wall:

$$\frac{[(T_{wall} - T)/T]_{LPP}}{[(T_{wall} - T)/T]_{\vartheta_1}} = \frac{[T_{wall} - T]_{LPP}}{[T_{wall} - T]_{\vartheta_1}}\left(\frac{\chi_{LPP}}{\chi_{\vartheta_1}}\right)^{\gamma-1} \tag{44}$$

If T_{IVC} represents the gas temperature at inlet valve closure, then the ratio between the temperature differences becomes:

$$\frac{[T_{wall} - T]_{LPP}}{[T_{wall} - T]_{\vartheta_1}} = \frac{T_{wall} - T_{IVC}\left(\frac{\chi_{IVC}}{\chi_{LPP}}\right)^{\gamma-1}}{T_{wall} - T_{IVC}\left(\frac{\chi_{IVC}}{\chi_{\vartheta_1}}\right)^{\gamma-1}} \tag{45}$$

Hence, from equations (38), (41), and (43)–(45), the entropy variations ratio can be evaluated by means of:

$$\frac{\delta S_{LPP}}{\delta S_{\vartheta_1}} = \left(\frac{\chi_{\vartheta_1}}{\chi_{LPP}}\right)^{\beta}\frac{[\chi + 1]_{LPP}}{[\chi + 1]_{\vartheta_1}}\frac{\left[T_{wall} - T_{IVC}\left(\frac{\chi_{IVC}}{\chi_{LPP}}\right)^{\gamma-1}\right]}{\left[T_{wall} - T_{IVC}\left(\frac{\chi_{IVC}}{\chi_{\vartheta_1}}\right)^{\gamma-1}\right]} \tag{46}$$

being the exponent $\beta = \gamma\,(a + b) - (b + c) - (\gamma - 1)$.

As can be noted, this ratio mainly depends on the engine geometry and on the heat transfer law, then for a given engine, it can be considered a constant:

$$\frac{\delta S_{LPP}}{\delta S_{\vartheta_1}} = \Phi \tag{47}$$

Assuming the values in Table 15 and taking into consideration three different heat transfer models (Woschni [7,8], Eichelberg [7,9] and Hohenberg [7]) it has been found that the values assumed by the ratio of equation (46) ranges from 1.81 to 2.05 according to the compression ratio and the engine heat transfer law, as shown in Fig. 15. A negligible dependence has been found with respect to the

Table 15

Compression ratios ρ	10 to 20
Rod to crank ratios μ	2.8 to 4.0
T_{wall}	70°C
T_{IVC}	40°C
γ	1.32
ϑ_{LPP}	−1

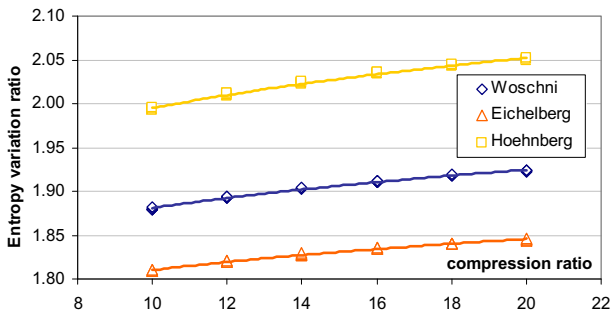

Fig. 15. Entropy variation ratio as function of compression ratio for three different heat transfer models

Table 16
Mean entropy variation ratio using three different heat transfer models.

Heat transfer model	a	b	c	Φ (mean value)
Woschni	0.8	−0.53	0	1.91
Eichelberg	0.5	0.50	0	1.83
Hohenberg	0.8	−0.40	−0.06	2.03

rod to crank ratio μ. The mean results obtained by each heat transfer model are resumed in Table 16, and, as can be noted, for the constant Φ a mean value equal to 1.92 could be adopted.

Thus the following relation can be assumed to calculate the loss function increment δF_{LPP} at the peak pressure position, once the δF_1 at the minimum $\delta V/V$ position has been evaluated:

$$\delta F_{LPP} \approx 1.92 \delta F_1 \tag{48}$$

This relation however has been derived for a constant mass process; it will be now shown that a similar relation can be derived in presence of mass leakage.

As shown in equation (10), for a real adiabatic evolution the loss function increment is:

$$\delta F = c_P \frac{\delta m}{m} \tag{49}$$

It follows that for an adiabatic process in presence of mass leakage (neglecting the specific heat change) the ratio of the loss function increment is:

$$\frac{\delta F_{LPP}}{\delta F_{\vartheta_1}} = \frac{\left[c_P \frac{\delta m}{m}\right]_{LPP}}{\left[c_P \frac{\delta m}{m}\right]_{\vartheta_1}} \approx \frac{\delta m_{LPP}}{\delta m_{\vartheta_1}} \frac{m_{\vartheta_1}}{m_{LPP}} \tag{50}$$

The mass escaping from cylinder through valve seats and piston rings during the crank rotation $\delta\vartheta$ (i.e. during the time interval δt) can be evaluated by means of the equation for the mass flow through a convergent nozzle. Once the gas pressure is above the critical pressure (which is about 2 times the outer pressure), the leakage mass is:

$$\delta m = -G_{nozzle}\delta t = -A_N \sqrt{k \cdot m \cdot \frac{p}{V}\left(\frac{2}{\gamma+1}\right)^{\frac{\gamma+1}{\gamma-1}}}\,\delta t \tag{51}$$

where A_N is the constant equivalent flow area. It follows that the ratio in equation (50) becomes:

$$\frac{\delta F_{LPP}}{\delta F_{\vartheta_1}} = \frac{\left[\sqrt{k \cdot m \cdot \frac{p}{V}\left(\frac{2}{\gamma+1}\right)^{\frac{k+1}{k-1}}}\right]_{LPP}}{\left[\sqrt{k \cdot m \cdot \frac{p}{V}\left(\frac{2}{\gamma+1}\right)^{\frac{k+1}{k-1}}}\right]_{\vartheta_1}} \frac{m_{\vartheta_1}}{m_{LPP}} \tag{52}$$

Assuming that during the rotation arc from ϑ_1 to TDC the isentropic coefficient k remains constant, the loss function ratio becomes:

$$\frac{\delta F_{LPP}}{\delta F_{\vartheta_1}} = \sqrt{\left[\frac{p}{m \cdot V}\right]_{LPP} \Big/ \left[\frac{p}{m \cdot V}\right]_{\vartheta_1}} \tag{53}$$

The mass escaped in the considered crank rotation arc can amount to few percentage points of the total mass, hence:

$$\sqrt{\frac{m_{\vartheta_1}}{m_{LPP}}} \approx 1 \tag{54}$$

Thus by means of the polytropic law pV^{γ} = constant and of the already introduced dimensionless variable $\chi = 2x/d$, the ratio in equation (53) becomes:

$$\frac{\delta F_{LPP}}{\delta F_{\vartheta_1}} = \left(\frac{\chi_{\vartheta_1}}{\chi_{LPP}}\right)^{\frac{\gamma+1}{2}} \tag{55}$$

Using the same values of Table 15 it was found that this ratio moves from 1.94 to 2.07, with a mean value of 2, which is not too far from the result obtained in the case of heat transfers and no mass leakage (see equation (48)), i.e. 1.92. Hence, considering a real diabatic process, the constant Φ should assume a value between 1.9 and 2, i.e. 1.95

References

[1] *428 TDC Sensor* at www.avl.com.
[2] *TDC sensor Type 2629B* at www.kistler.com.
[3] Ylva Nilsson, Lars Eriksson, "Determining TDC Position Using Symmetry and Other Methods", SAE Paper 2004-01-1458.
[4] Mitsue Morishita, Kushiyama Tadashi, "An Improved Method for Determining the TDC Position in a PV Diagram", SAE Paper 980625.
[5] A. Hribernik, "Statistical Determination of Correlation Between Pressure and Crankshaft Angle During Indication of Combustion Engines", SAE Paper 982541.
[6] Marek J. Stas, "Thermodynamic Determination of T.D.C. in Piston Combustion Engines", SAE Paper 960610.
[7] C.A. Finol, K. Robinson, Thermal modelling of modern engines: a review of empirical correlations to estimate the in-cylinder heat transfer coefficient. Proceedings of the Institution of Mechanical Engineers, Part D: Journal of Automobile Engineering 220 (2006).
[8] J.I. Ramos, Internal Combustion Engine Modeling. Hemisphere Publishing Corporation, 1989.
[9] J.H. Horlock, D.E. Winterbone, The Thermodynamics and Gas Dynamics of Internal Combustion Engines, vol. II, Clarendon Press, Oxford, 1986.
[10] Randolph Andrew L., "Methods of processing cylinder-pressure transducer signals to maximize data accuracy", SAE Paper 900170.
[11] Brunt Michael F.J., Pond Christopher R., "Evaluation of techniques for absolute cylinder pressure correction", SAE Paper 970036.

Symbols and abbreviations

A: in-cylinder heat exchange surface area
Ac: cylinder section area = $(\pi d^2)/4$
A_N: equivalent nozzle flow area for mass leakage calculation
c: engine stroke
c_P: constant pressure specific heat of the gas
c_V: constant volume specific heat of the gas
d: piston bore
dY: differential of the generic function *Y*
$error_T$: gas temperature uncertainty at inlet valve closure
$error_\rho$: engine compression ratio uncertainty
F: loss function
h: heat exchange coefficient
k: gas isentropic coefficient = c_P/c_V
l: rod length
m: in-cylinder gas mass
p: in-cylinder gas pressure
p': in-cylinder gas pressure affected by measurement errors
Q: heat received by the gas from the cylinder walls
q: specific heat received by the gas from the cylinder walls
r: crank radius
R': in-cylinder gas constant
S: in-cylinder gas specific entropy
T: in-cylinder gas temperature
t: time
T_{wall}: cylinder walls temperature
u: in-cylinder gas specific internal energy
u_m: mean piston speed
v: in-cylinder gas specific volume
V: in-cylinder volume
x: piston distance from the cylinder top
z: crank pin offset
χ: adimensional piston position = $2x/d$
$\delta F_1 = \delta F_{min\ dV/V}$: loss function increment at the minimum dV/V angle
$\delta F_2 = \delta F_{max\ dV/V}$: loss function increment at the maximum dV/V angle
δF_{LPP}: loss function increment at the peak pressure position
δF_m: mean loss function increment = $1/2\,(\delta F_1 + \delta F_2)$
δt: time interval during the elementary crank rotation $\delta\vartheta$
δY: finite increment of the generic function *Y* during the elementary crank rotation $\delta\vartheta$
Φ: proportionality constant
γ: exponent of the polytropic evolution
μ: engine rod to crank ratio
ϑ: crank position
ϑ_1: crank position for the minimum dV/V

ϑ_2: crank position for the maximum dV/V
ϑ_B: BDC crank position measured with respect to cylinder axis (non centred crank mechanism)
ϑ_{loss}: loss angle
ϑ_T: TDC crank position measured with respect to cylinder axis (non centred crank mechanism)
ρ: engine compression ratio
τ: adimensional crank pin offset $= z/l$
ATDC: after top dead centre
BDC: bottom dead centre
BTDC: before top dead centre
CA: crank angle
CAD: crank angle degree(s)
IMEP: indicated mean effective pressure
IVC: inlet valve closure
LPP: location of pressure peak
LTDC: location of top dead centre
MAP: manifold absolute pressure
TDC: top dead centre